IAC-22,C2,3,12,x68485

Estimation of a Craig-Bampton Equivalent Model using a hybrid Particle Swarm Optimization for DCLA purposes

Corinna Cerini[a*] **and Guglielmo S. Aglietti**[a]

[a] *Te Pūnaha Ātea - Space Institute, University of Auckland, Auckland, 1010, New Zealand*

Abstract

It is common practice in industry to deliver a Craig-Bampton (CB) reduced version of the SpaceCraft (S/C) Finite Element Model (FEM) to the launch authorities to perform the Dynamic Coupled Load Analysis (DCLA). During the DCLA, the FEM of the S/C is coupled with the FEM of the Launch Vehicle (LV) to predict the responses caused by the vibration environment produced during the launch phases (e.g., lift-off, engine start-up, etc.). Before being CB-reduced, the FEM needs to be correlated and validated against physical test results to guarantee its capability to reproduce the actual behaviour of the physical hardware, which is essential to perform a meaningful DCLA. Given the complexity and size of the FEM, the entire process can be very demanding. In this paper, an alternative to the mathematical models usually used in the DCLA is investigated. The main idea is to synthesize a Craig-Bampton equivalent model directly from the response data of a vibration test experiment. The system identification problem is solved using a Particle Swarm Optimization (PSO) algorithm, tailored specifically for this type of application, the hybrid PSO and Local Search (hPSO-LS). A mutation operator from Genetic Algorithm (GA) is used to improve the solution and the local search method to refine the final result. The proposed method is numerically tested on a 5-Degree of Freedoms (DoFs) lumped mass system, with full stiffness and damping matrices. A sensitivity analysis of the search space size is also carried out to investigate its influence on the final results. The hPSO-LS is tested in both noise-free and noisy scenarios.

Keywords: Testing, System Identification, Dynamic Coupled Load Analysis, Particle Swarm Optimization

Abbreviations

APSO	Adaptive PSO
CB	Craig-Bampton
CLA	Coupled Load Analysis
CMS	Component Mode Synthesis
COC	Cross Orthogonality Check
DCLA	Dynamic Coupled Load Analysis
DoF	Degree of Freedom
EA	Evoluationary Algorithm
ECSS	European Cooperation for Space Standardization
ESE	Evolutionary State Estimation
FEM	Finite Element Model
GA	Genetic Algorithm
hPSO-LS	hybrid PSO and Local Search
LS	Local Search
LV	Launch Vehicle
MAC	Modal Assurance Criterion
NIA	Nature-Inspired Algorithm
PSO	Particle Swarm Optimization
S/C	SpaceCraft
SBA	Swarm-Based Algorithm
SI	Swarm Intelligence

1. Introduction

The Dynamic Coupled Load Analysis (DCLA) is a crucial task in the design and verification phase of a SpaceCraft (S/C). Its main goal is to calculate the mechanical environment due to dynamic loads caused by the launch transients and is carried out as part of the mission analysis. Depending on the status of the project, the DCLA, also called the Coupled Load Analysis (CLA), can be either a single indicator of compliance or an integrated tool in a S/C structure's design process. In both cases, the S/C and the Launch Vehicle (LV) substructure mathematical models must be reduced and then merged together to perform transient and harmonic dynamic analyses in the low-frequency range (from 0 to 100 Hz), applying the various launch events' forcing functions. To accomplish that, several reduction methods have been developed over the last decades. These methods are referred to as the Component Mode Synthesis (CMS) and can be subdivided into fixed-interface and free-interface methods, depending on the boundary conditions [1]. Generally, to dynamically reduce the S/C mathematical model, the fixed interface Craig-Bampton (CB) method is used [2]. In this paper, the possibility of obtaining an equivalent CB mathematical model of a generic structure dir-

ectly from some experimental data (the nature of those is clarified in the next sections) is explored.

In literature, the process of derivation of a mathematical model from the experiments is known as system identification [3] and it can be classified as an *inverse* problem. Following the categories mentioned by Bekey in [4], the problem introduced in the present paper, is more specifically identified as a *modelling* problem: "given a set of inputs and corresponding outputs from a system, find a mathematical description of the system" [5]. Problems of this kind can be addressed using optimization techniques. The selection of a method for a particular application depends on the nature of the problem and what is desired. Traditional methods, such as gradient-based optimization algorithms, may not be suitable to address some complicated engineering problems, e.g., multimodal, non-convex, and large-scale. Moreover, they require a good initial guess to start the process. The problem can be very sensitive to the choice of these estimates, which makes them difficult to apply if no a priori knowledge is available. Modern Nature-Inspired Algorithm (NIA)s have been found to be effective at generating optimal or near-optimal solutions for these types of problems. Among these new generations of NIAs, the Evoluationary Algorithm (EA)s and the Swarm-Based Algorithm (SBA)s have emerged to be the most promising, and they have been successfully applied in system identification problems. The idea of Swarm Intelligence (SI) derives from the collective behavior of scattered and self-organized systems. Its incorporation into the optimization methods led to the arrival of the SBAs. Among them, the Particle Swarm Optimization (PSO) [6,7] has found to be the most representative SI method. In fact, the PSO has been successfully used to address problems of different nature in the engineering structural field, such as structural reliability assessment [8], structural design optimization [9–11] and composite structure optimization [12], as well as system identification and parameter estimation [13]. Specifically for the identification of the spatial properties of a structure, various methodologies have been proposed in noise-free and noisy scenarios. Common ground for all them is the type of experimental data available: output accelerations and input forces. In [14] a EA is adopted to solve the identification problem of a three Degree of Freedoms (DoFs) lumped mass system if no prior knowledge of mass, damping or stiffness is available, but increasing the number of DoFs, the mass distribution is assumed to be known. Some techniques also combine the EA with a Local Search (LS) to accelerate the convergence to the optima points [15]. Large structural systems have also been tested, assuming the mass matrix to be known, as well as the coefficient to define the proportional damping matrix [16]. In [17], a PSO strategy is used to solve identification problem for a two and ten DoFs system. It is shown that the performance of PSO is slightly better than Genetic Algorithm (GA). Moreover, a damping model, e.g., proportional damping, has been selected in all these methods.

To the best of the author's knowledge, no technique presently available in literature is capable of solving the identification problem using only output and input accelerations. This study aims to tailor the well-known PSO for the specific task of synthesizing a mathematical model that can be used as an alternative to the currently used CB reduced Finite Element Model (FEM). Around the PSO logic, the hybrid PSO and Local Search (hPSO-LS) is built. This multistage algorithm is developed in MATLAB: the exhaustive exploration of the search space is delegated to the global phase, and the final adjustment or refining to the local phase.

2. Background and preliminaries

The excitation induced by the launcher on a spacecraft structure can be seen like the motion of the support (or shaker table). In this paper, the case of a single-axis excitation is considered. The structure *'s'* is accelerated at its base *'b'* by a seismic excitation of acceleration $\ddot{u}_b$ and absolute accelerations are measured. The system may be considered as placed on a fictitious shaking table excited by an unknown force, but a known acceleration $\left\{\ddot{u}_b\right\}$. While this hypothesis could be released, as the force could be measured, this paper investigates the identification with accelerations only.

The synthesized mathematical model should describe the dynamic behaviour of the structure in the frequency range of interest. To assess the quality of it, this paper refers to the correlation criteria established by European Cooperation for Space Standardization (ECSS) [18] and shown in Table 1. They are defined as follows, with the subscript *t* for target, and *e* for estimated:

- Eigenfrequency deviation.

$$f_i^{\text{error}} = 100\frac{f_i^t - f_i^e}{f_i^e} \tag{1}$$

  where f_i is the i-th natural frequency. The superscript t refers to the natural frequencies obtained from the target system and *e* to the ones obtained from the optimized system.

- Modal Assurance Criterion (MAC): measure of the degree of correlation between two mode shapes ϕ_e and ϕ_t.

$$\text{MAC}_{et} = \frac{\left[\left\{\phi\right\}_e^T \left\{\phi\right\}_t\right]^2}{\left[\left\{\phi\right\}_e^T \left\{\phi\right\}_e\right]\left[\left\{\phi\right\}_t^T \left\{\phi\right\}_t\right]} \tag{2}$$

- Cross Orthogonality Check (COC): measure of the mathematical orthogonality of mode shapes ϕ_t (tar-

get) and ϕ_e (estimated) with respect to the numerical mass matrix M_t.

$$\text{COC}_{et} = \frac{\{\phi\}_e^T [M_t] \{\phi\}_t}{\sqrt{\{\phi\}_e^T [M_t] \{\phi\}_e} \sqrt{\{\phi\}_t^T [M_t] \{\phi\}_t}} \tag{3}$$

Note that these criteria were established for correlation between numerical, i.e., a FEM, and experimental results. Therefore, they are here considered only as a reference to assess the validity of the proposed methodology.

Before getting into the formulation of the problem, it is necessary to introduce the CB reduced model and its mathematical derivation.

2.1 Craig-Bampton

The equations of motion of linear dynamic systems can be written in physical coordinates as:

$$\begin{bmatrix} M_{LL} & M_{LR} \\ M_{RL} & M_{RR} \end{bmatrix} \begin{Bmatrix} \ddot{u}_L \\ \ddot{u}_R \end{Bmatrix} + \begin{bmatrix} C_{LL} & C_{LR} \\ C_{RL} & C_{RR} \end{bmatrix} \begin{Bmatrix} \dot{u}_L \\ \dot{u}_R \end{Bmatrix} + \begin{bmatrix} K_{LL} & K_{LR} \\ K_{RL} & K_{RR} \end{bmatrix} \begin{Bmatrix} u_L \\ u_R \end{Bmatrix} = \begin{Bmatrix} F_L \\ F_R \end{Bmatrix} \tag{4}$$

where the *subset L* contains the internal DoFs and the *subset R* the fixed, boundaries and retained DoFs. The input forces F_L applied to the internal DoFs are zero. In the transformation process, the *subset L* is converted to modal coordinates and it is then truncated to a smaller set *m* (number of retained DoFs). The new hybrid coordinates are related to the initial physical coordinates as follows:

$$\begin{Bmatrix} u_L \\ u_R \end{Bmatrix} = \begin{bmatrix} \phi_L & \phi_R \\ 0 & I \end{bmatrix} \begin{Bmatrix} q_m \\ u_R \end{Bmatrix} \tag{5}$$

where ϕ_R is the (L x R) matrix of the constraint modes, ϕ_L is the (L x m) matrix of the normal mode shapes with fixed boundary condition.

The CB-reduced mass, stiffness and damping matrices can be expressed respectively as:

$$M_{\text{CB}} = \begin{bmatrix} M_{mm} & M_{mB} \\ M_{Bm} & M_{BB} \end{bmatrix} \tag{6}$$

$$K_{\text{CB}} = \begin{bmatrix} K_{mm} & 0 \\ 0 & K_{BB} \end{bmatrix} \tag{7}$$

$$C_{\text{CB}} = \begin{bmatrix} C_{mm} & 0 \\ 0 & C_{BB} \end{bmatrix} \tag{8}$$

where the terms in Eq. (6) are:

$$\begin{aligned} M_{BB} =& M_{RR} + M_{RL}\phi_R + \phi_R^T M_{LR} + \phi_R^T M_{LL}\phi_R \\ M_{mm} =& \phi_L^T M_{LL}\phi_L = \mu \\ M_{Bm} =& M_{mB}^T = [M_{RL} + \phi_R^T M_{LL}] \end{aligned} \tag{9}$$

$M_{mm} = \mu$ is the generalized mass matrix.

Terms in Eqs. (7) and (8) are:

$$\begin{aligned} K_{mm} =& \phi_L^T K_{LL}\phi_L = \mu\omega_0^2 \\ C_{mm} =& 2\zeta\mu\omega_0 \end{aligned} \tag{10}$$

ω_0^2 is the diagonal matrix of the eigenvalues, ζ is the critical damping ratio. K_{BB} and C_{BB} are zero for statically determinant interfaces.

2.2 Mathematical Formulation

The partitioning of the DoFs and therefore the transformation matrix used to formulate the CB equivalent model is slightly different from Eq. (5). Since the structural vibrations occur as motions relative to the rigid-body movements, it is necessary to divide displacements, velocities, and accelerations into their absolute and relative components. The required linearized kinematic relation is shown in [19, 20] and leads to:

$$\{\ddot{u}_s\} = \{\ddot{v}_s\} + [G]\{\ddot{u}_b\} \tag{11}$$

where $[G]$ is a time-independent geometry matrix that can be interpreted as rigid body displacements due to the translational and rotational base motions. $\{\ddot{u}_s\}$ is the absolute acceleration vector for all the structural points, $\{\ddot{v}_s\}$ is the relative acceleration vector and $\{\ddot{u}_b\}$ is the base acceleration vector.

The *s-set* is referred to all the measured physical DoFs on the structure. The *b-set* is the physical DoF where the input is applied. Note that in the present formulation, the *subset L* and part of the *subset R* of the CB model are included in the *s-set*. Therefore the equations of motion result as follows:

$$\begin{bmatrix} M_{ss} & M_{sb} \\ M_{bs} & M_{bb} \end{bmatrix} \begin{Bmatrix} \ddot{u}_s \\ \ddot{u}_b \end{Bmatrix} + \begin{bmatrix} C_{ss} & C_{sb} \\ C_{bs} & C_{bb} \end{bmatrix} \begin{Bmatrix} \dot{u}_s \\ \dot{u}_b \end{Bmatrix} + \begin{bmatrix} K_{ss} & K_{sb} \\ K_{bs} & K_{bb} \end{bmatrix} \begin{Bmatrix} u_s \\ u_b \end{Bmatrix} = \begin{Bmatrix} F_s \\ F_b \end{Bmatrix} \tag{12}$$

It is assumed that the DoFs related to both the structure and base can be modelled by lumped masses, i.e., $[M_{sb}] = [0]$ and $[M_{bs}] = [0]$. It is also assumed that the base is stiff, i.e., $\{v_b\} = \{0\}$, and that there are not external forces $\{F_s\}$ acting on the structure. The equation of interest for the *s-set* can be derived from Eqs. (11) and (12) and it results in:

$$[M_{ss}]\{\ddot{v}_s\} + [C_{ss}]\{\dot{v}_s\} + [K_{ss}]\{v_s\} = -[M_{ss}][G]\{\ddot{u}_b\} \tag{13}$$

This equation shows that the structural vibrations are induced by inertia forces which are caused by the multi-axial base excitation $\{\ddot{u}_b\}$.

Table 1. Test-analysis correlation criteria, ECSS [18]

Item	Quality Criterion	
Fundamental bending modes of a S/C	MAC: Eigenfrequency deviation:	> 0.9 $< 3\%$
Modes with effective masses $> 10\%$ of the total mass	MAC: Eigenfrequency deviation:	> 0.85 $< 5\%$
For other modes in the relevant frequency range	MAC: Eigenfrequency deviation:	> 0.8 $< 10\%$
Cross-orthogonality check	Diagonal terms: Off-diagonal terms:	> 0.9 < 0.10

In Section 4, the mathematical formulation is formalized for a single-axis excitation, but it can be expanded for a more general case. Note that the Eq. (13) is expressed in physical coordinates, whereas the CB model is built in hybrid coordinates, i.e., physical and modal coordinates.

3. Particle Swarm Optimization Algorithm

The first PSO algorithm has been introduced by Kennedy and Eberhart in [6, 7]. The idea comes from the behaviour of fish schooling and bird flocking. Birds and fish adjust their movements to avoid predators, seek food, optimize environmental parameters, etc. Potential solutions in the PSO are called *particles*. Contrary to the individuals of the GA [21], the particles do not compete with each other, but share helpful information. At each iteration *t*, each particle *n* is associated with the vector of the *current position* and *current velocity*, $\{P_t^n\}$ and $\{V_t^n\}$ respectively:

$$\begin{aligned} \{P_t^n\} &= \{p_t^{n,1}, p_t^{n,2}, ..., p_t^{n,D}\} \\ \{V_t^n\} &= \{v_t^{n,1}, v_t^{n,2}, ..., v_t^{n,D}\} \end{aligned} \tag{14}$$

Each particle keeps track of the best position it has visited so far, the so-called *local attractor* or *personal best*, $L_t^{n,d}$, as well as the global best position so far achieved by the swarm, the so-called *global attractor* or *global best*, G_t^n. During their journey, the velocity in the next iteration, is computed as a function of the best position of the swarm, the best personal position and its previous velocity. The movement of the particles, in terms of velocity and position, is governed by the following equations:

$$V_{t+1}^{n,d} = \omega V_t^{n,d} + c_1 r_t^{n,d} \left(L_t^{n,d} - P_t^n\right) + c_2 s_t^{n,d} \left(G_t^n - P_t^n\right) \tag{15}$$

$$P_{t+1}^{n,d} = P_t^{n,d} + V_{t+1}^{n,d} \tag{16}$$

where *t* defines the iteration, *n* the number of the particle that is moved and *d* the component. The swarm is then responding by the combination of the quality factors $L_t^{n,d}$ and G_t^n, weighted by the constants c_1 and c_2, called *personal acceleration coefficient* and *social acceleration coefficient* respectively [7]. They control the influence of the personal memory of a particle and the common knowledge of the swarm. Some randomness is added using $r_t^{n,d}$ and $s_t^{n,d}$, which are drawn uniformly at random in [0,1] and are all independent of each other [6]. The so-called *inertia weight* ω [22, 23], is introduced in the updating equation to avoid the phenomenon of *explosion* [24]. Therefore, the second and third term of the updating equation of the velocity in Eq. (15) can be seen as and external force F_t acting on the particle, then the acceleration of the particle can be written as $\Delta V_t = F_t - (1-\omega)V_t$, and so ω can be interpreted as the fluidity of the medium in which the particle moves. The representation of the PSO model is shown in Fig. 1. By adjusting the parameters ω, c_1 and c_2, it is possible to influence the trade-off between the *exploration* (the capability to search in areas that have not been visited before) and the *exploitation* (the capability to refine already good search points). Experiments have shown that both acceleration coefficients are essential to the success of the PSO [25], as well as the inertia coefficient. Among all the existing strategies, the most promising to optimally control these coefficients, seems to be the adaptation technique based on the Evolutionary State Estimation (ESE) and presented in [26], the Adaptive PSO (APSO). During the iterations, the population distribution varies, as well as the information it carries. The APSO uses this information to estimate the evolutionary state of the process, subsequently used to adapt the accelerations coefficients. The inertia weight changes according to the distribution of the particles.

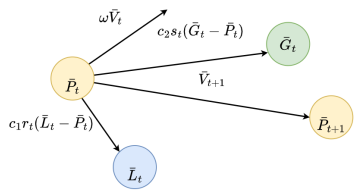

Fig. 1. Schematic illustration of the particle's dynamics

The concept of ESE was first introduced in [27, 28], where, instead of having a fixed probabilities of crossover and mutation, the evolutionary state was used to vary them accordingly. Evolution state is defined as one the states that a particle might be in, depending on which one, the following strategies are adopted:

- *Exploration:* it is important to explore as many optima as possible, hence increasing c_1 and decreasing c_2 can help particles explore individually and achieve their own historical best position.
- *Exploitation:* the particles are making use of local information and grouping toward possible local optimal regions indicated by the best personal position visited so far. c_1 is increased and c_2 slightly decreased.
- *Convergence:* the swarm seems to find the globally optimal region; hence, c_2 is slightly increased to lead other particles to the probable globally optimal region and c_1 should is slightly decreased to let the swarm converge fast.
- *Jumping out:* the global best particle is jumping out of a local optimum toward a better optimum; therefore a large c_2 together with a relatively small c_1 is set.

4. Proposed algorithm

The hPSO-LS is divided in two main steps: the *Global Phase* and *Local Phase*. The *Global Phase* implements the adaption of the acceleration and inertia coefficients of the APSO. The mutation operator from the GA is also used on the Global Best to explore better solutions, as well as on some particles as a 'healing process'. The *Local Phase* focuses on finding the local minimum in the basin of attraction given by the Global Best of the previous phase.

4.1 Problem Statement

The identification of mass, stiffness and damping matrices of the system under consideration is obtained by solving a minimization problem in the frequency domain. Hence, Eq. (13) is transformed into the frequency domain by use of the steady state response solution, in case of harmonic excitation. The transformation yields:

$$\begin{aligned}\left(-\omega^2\left[M_{SS}\right]+j\omega\left[C_{SS}\right]+\left[K_{SS}\right]\right)\left\{\ddot{v}_s\right\}=\\ \omega^2\left[M_{SS}\right]\left[G\right]\left\{\ddot{u}_b\right\}\end{aligned} \tag{17}$$

The following identification equation is used to build the cost function:

$$\begin{aligned}-\left[M_{ss}\right]\left[\ddot{V}_s\right]\left[\Omega^2\right]+j\left[C_{ss}\right]\left[\ddot{V}_s\right]\left[\Omega\right]+\\ +\left[K_{ss}\right]\left[\ddot{V}_s\right]=\left[M_{ss}\right]\left[G\right]\left[\ddot{U}_b\right]\left[\Omega^2\right]\end{aligned} \tag{18}$$

where $\left[\ddot{V}_s\right]$ is the n by n_f matrix of the relative accelerations, with n number of physical DoFs, e.g., number of measuring locations, and n_f number of excitation frequencies. $\left[\Omega\right]$ is the n_f by n_f diagonal excitation frequency matrix and j is the imaginary number. The entries of the mass, stiffness and damping matrices are grouped in a vector $\mathbf{x}=\{x_d\}$, for $d=1,2,\ldots,D$. Define a function $\mathcal{F}(x)$ as:

$$\begin{aligned}\mathcal{F}(x)=-\left[M_{ss}(x)\right]\left[\ddot{V}_s\right]\left[\Omega^2\right]+j\left[C_{ss}(x)\right]\left[\ddot{V}_s\right]\left[\Omega\right]+\\ +\left[K_{ss}(x)\right]\left[\ddot{V}_s\right]-\left[M_{ss}(x)\right]\left[G\right]\left[\ddot{U}_b\right]\left[\Omega^2\right]\end{aligned} \tag{19}$$

The optimization problem requires finding a vector $\mathbf{x}\in\mathcal{S}$, where $\mathcal{S}$ is the search space, so that the error norm of $\mathcal{F}$:$\mathcal{S}\rightarrow\mathbb{R}$, defined in Eq. (20), is minimized.

$$\|\mathcal{F}\|=\sqrt{\sum_{i=1}^{n}\sum_{j=1}^{n_f}\mid f_{ij}\mid^2} \tag{20}$$

The solution of the minimization term will be called $\mathbf{x}_*$ if $\mathcal{F}(\mathbf{x}_*)$ is the global minimum of $\mathcal{F}$ in $\mathcal{S}$, or:

$$\mathbf{x}_*\in\mathcal{S}\quad\mid\quad\mathcal{F}(\mathbf{x}_*)\leq\mathcal{F}(\mathbf{x})\quad\forall\mathbf{x}\in\mathcal{S} \tag{21}$$

The search space $\mathcal{S}$ is defined by a set of maximum and minimum values that the parameters can assume. It consist in two vectors of size D values, $\mathbf{x}_{max}$ and $\mathbf{x}_{min}$, respectively, such that:

$$\mathcal{S}=\left\{\mathbf{x}\in\mathbb{R}^D|\mathbf{x}_{min,d}\leq\mathbf{x}_d\leq\mathbf{x}_{max,d}\quad\forall d\in1,2,\ldots,D\right\} \tag{22}$$

Not all the particles in the search space might provide physically plausible solutions. The physically possible solutions are a subset of the obtainable values of the parameters in $\mathcal{S}$. However, restricting the search space to the feasible region is almost impossible, given the nature of the constrictions. Therefore a strategy is implemented a strategy to prevent the particle from following non-physical solutions, starting from the settings of the initial swarm. Specifically, the constraints taken into account are:

- Total mass of the structure
- Symmetry of the stiffness and damping matrices
- Positive definiteness of the mass matrix
- Semi-positive definiteness of the stiffness matrix

The first two constraints are easy to handle since they can be considered built-in within the formulation of the cost function. Both help to reduce the number of variables. The total mass constraint allows considering *4* unknowns instead of *5* in the mass matrix. The symmetry of the stiffness and damping matrices reduces the variables from *25*

to *15* in each matrix. Regarding the positive and semi-positive definiteness, the implemented strategy is different in the *Global* and *Local Phase*. In the first part of the algorithm, a label is assigned to each particle of the initial swarm, stating its status of 'health'. In Section 4.3 it is shown how this information is used to drive the process. General settings for the Global and Local Phases are shown in Table 2.

Table 2. Parameters setting for Global Phase and Local Phase

Parameter	Global Phase
Initial c_1	2
Initial c_2	2
Initial w	0.9
Mutation Rate μ	0.4
Swarm Size *N*	100
Max. Iterations	5000
Parameter	**Local Phase**
Max. Iterations	1000
Step Tolerance	1e-16
Constraint Tolerance	1e-2

4.2 Global Phase: Initialization Strategy

The first step of the iterative process starts with the initialization of the swarm, or population. Recall that **x** is the vector of *D* parameters, corresponding to the entries of the mass, stiffness and damping matrices. These entries are grouped in *P* (see Eq. (16)), representing the position of the particle in the search space. The initialization is carried out picking *N* particles at random from $\mathcal{S}$, so that the initial swarm is defined by:

$$P = \mathbf{x}_{min} + R(\mathbf{x}_{max} - \mathbf{x}_{min}) \tag{23}$$

R denotes a realisation of uniformly distributed random variable in the interval [0,1] that is sampled for each parameter *d* individually ($d = 1, 2, \ldots, D$). The number *N* of particles defines the size of the swarm and it is kept fixed to 100 during the iterations.

4.3 Global Phase: Main

The core of the proposed algorithm is developed around the APSO. Hence, the acceleration coefficients are adjusted during the iteration according to the evolutionary state, as summarized in Table 3. The inertia weight is instead updated based on the population distribution. Initial values of these coefficients, as well as the number of particles and the maximum iterations are shown in Table 2.

Table 3. Adaptation strategies for the variation of the acceleration coefficients c_1 and c_2, [26]

State	c_1	c_2
Exploration	Increase	Decrease
Exploitation	Increase slightly	Decrease slightly
Convergence	Increase slightly	Increase slightly
Jumping-out	Decrease	Increase

Each particle is labelled to keep record of its *'health'* status. Depending on which constraint fails, the label might refer to the mass or stiffness matrices. Hence, a *'healing process'* is implemented. If the components of the particle related to either the mass or stiffness fail to respect the constraints, the particle is marked as *'sick'*. Following the spirit of cooperation among the swarm members, the mutation operator is here applied to heal the *'sick'* particles. Hence, it can be considered as a targeted mutation, operating only on the entries that make the particle *'sick'*. A mutation rate μ of 0.4 defines the mutation probability: high genetic variation in the beginning to 'heal' as many particles as possible, and as the algorithm approaches the end, it is probable that the algorithm has entered the convergence phase, in which the particles are all gathered around the Global Best. Note that only *'healthy'* particles can be considered for the updating of the Global Best. The mutation is also applied on the Global Best when it gets stuck in a local minimum. The idea is to give it a push to improve itself.

Although the evaluation of the cost function is the most used termination criteria, it is unlikely to achieve a very low cost function, especially with noise-corrupted data. Therefore, a maximum number of iterations is allowed, and set here to 5000. Moreover, in order to accelerate the process, an eigenproblem is solved every 200 iterations with the current Global Best to check the quality of the solution in terms of natural frequencies in the frequency range of interest. If satisfactory results are achieved, the Global Phase stops, and the Local Phase starts. The quality on the solution is given by the presence of *m* modal DoFs, with *m* being the number of the expected natural frequencies in the considered frequency range, and a 5% of deviation is allowed.

4.4 Local Phase: Refining Solution

The Local Search is the last part of the algorithm, in which the Global Best found in the previous phase, the G_N, is given as an initial guess to an *interior-point* constrained convex optimizer for the final refining of the solution [29]. The MATLAB implementation of this al-

gorithm is here used with the function *fmincon*[1]. The function *nonlcon* is used to handle the constraints previously mentioned.

5. Numerical experiments

A 5-DoFs system with lumped masses and full stiffness and damping matrices is considered. No damping model is assumed to be known; therefore, the algorithm aims to find the damping matrix's entries directly. The structure is assumed to be excited by a known acceleration at the base, and five output accelerations are measured. The system's dynamics are modelled by Eq. (13). The entries of the matrices $[M_{SS}]$, $[C_{SS}]$ and $[K_{SS}]$ define the set of parameters that fully describes the system:

$$\{x\} = \begin{Bmatrix} m_{11}, m_{22}, m_{33}, m_{44}, k_{11}, k_{12}, k_{13}, k_{14}, \\ k_{15}, k_{22}, k_{23}, k_{24}, k_{25}, k_{33}, k_{34}, k_{35}, k_{44}, \\ k_{45}, k_{55}, c_{11}, c_{12}, c_{13}, c_{14}, c_{15}, c_{22}, c_{23}, \\ c_{24}, c_{25}, c_{33}, c_{34}, c_{35}, c_{44}, c_{45}, c_{55} \end{Bmatrix} \tag{24}$$

Call *M* the total mass of the structure, the last entry in the diagonal mass matrix is set to:

$$m_{55} = M - (m_{11} + m_{22} + m_{33} + m_{44}) \tag{25}$$

For a total of system variables of *34*.

The definition of the search space is not trivial, especially in a real case situation where no prior knowledge of the system is available, and only guesses are possible. The search space influences the evolutive process since it might or might not include a local minimum in a constrained optimisation problem. Moreover, assuming that local minima are included, the search space size influences the paths a particle can take to get to a local minimum. Therefore, a sensitivity analysis of the search space is carried out as a side study to understand whether or not a large space might influence the final result.

A search space, as described in Eq. (22), is defined by the two vectors of the lower and upper plausible values that the particle position can assume during the iterations, and successively in the refining process. Two test cases are considered, *Case 1* and *Case 2*. Concerning the bounds of the mass matrix entries, no differences are implemented between the two cases since $\mathbf{x}_{min}$ values are kept to 0 and $\mathbf{x}_{max}$ values are set equal to the total mass of the structure, which is always part of the a priori knowledge. Upper and lower bounds of the stiffness and damping matrices are instead defined based on the desired solution $\mathbf{x}_*$ as follows:

- $\mathbf{x}_{max}$ = 3$\mathbf{x}_*$ for *Case 1* and $\mathbf{x}_{max}$ = 7$\mathbf{x}_*$ for *Case 2*
- $\mathbf{x}_{min}$ = -$\mathbf{x}_{max}$ for *Case 1* and *Case 2*

Both cases are considered in noise-free and noisy scenarios. Given the stochastic nature of the adopted method, 20 independent runs are performed for each test case to show its effectiveness, and their mean and maximum results are used in the comparison. All the experiments are carried out on the same machine with an Intel(R) Core(TM) i7-9700 CPU 3.00 GHz, 32 GB memory and Windows 10 operating system. The average CPU time for a noise-free simulation is 600 s, whereas for a simulation using noise-corrupted data, it is 900 s.

5.1 Noise-free scenario

Increasing the search space is not necessarily a deficit for the optimization problem. Tables 4 and 5 show the mean and maximum errors over the 20 runs for mass and stiffness entries, respectively. The maximum absolute errors are listed below:

- Max. absolute error of the mass entries is 1.08% for *Case 1* and 1.04% for *Case 2*
- Max. absolute error of the stiffness entries is 1.15% for *Case 1* and 1.11% for *Case 2*

The absolute errors for the mass and the stiffness variables are comparable, as well as the results for *Case 1* and *Case 2*. Given the minor errors on the entries of the mass and stiffness matrices, the solution of the undamped eigenproblem results in a maximum deviation of the first natural frequency of 0.07% for *Case 1* and *Case 2*. The errors on the other frequencies are negligible.

The damping matrix gives slightly larger errors compared to the mass and stiffness's, but for the ninth variable c_{25} (= c_{52}) (see Table 6). Its maximum absolute error is two orders of magnitude bigger than the other entries in that matrix. The mean maximum error is 10.17% and 25.72%, for *Case 1* and *Case 2*, respectively. Further studies must be conducted to investigate if the large error observed for c_{25} is a problem-related situation. However, the damping matrix is generally considered in a modal environment, or a model is assumed a priori, e.g., proportional damping. Whether or not the implementation of such a model may improve the accuracy of the solution will be analysed in future works. The results of the damped eigenproblem are shown in Table 7. Although the large maximum errors observed in that specific entry of the damping matrix, the maximum damping deviation does not exceed 0.84% for *Case 1* and 1.85% for *Case 2*. However, the large errors observed in *Case 2* compared to *Case 1*, result in a larger damping deviation, although contained. The eigenfrequencies deviation shows the same situation as for the undamped problem.

The identification results for *Case 1* and *Case 2* are summarized in Fig. 2, where the ratios of the estimated

[1] fmincon is a non-linear programming solver implemented in MATLAB which finds the minimum of constrained non-linear multivariate function

Table 4. Mean and maximum absolute error on the mass entries of 20 runs for *Case 1* ($\mathbf{x}_{max} = 3\mathbf{x}_*$) and *Case 2* ($\mathbf{x}_{max} = 7\mathbf{x}_*$)

Variable	Mean Value (%)		Max. Value (%)	
	Case 1	*Case 2*	*Case 1*	*Case 2*
m_{11}	0.64	0.66	0.94	0.91
m_{22}	0.66	0.68	0.98	0.94
m_{33}	0.32	0.33	0.46	0.49
m_{44}	0.76	0.75	1.08	1.04

Table 5. Mean and maximum absolute error on the stiffness entries of 20 runs for *Case 1* ($\mathbf{x}_{max} = 3\mathbf{x}_*$) and *Case 2* ($\mathbf{x}_{max} = 7\mathbf{x}_*$)

Variable	Mean Value (%)		Max. Value (%)	
	Case 1	*Case 2*	*Case 1*	*Case 2*
k_{11}	0.64	0.66	0.94	0.91
$k_{12} = k_{21}$	0.66	0.68	0.97	0.95
$k_{13} = k_{31}$	0.49	0.50	0.70	0.71
$k_{14} = k_{41}$	0.43	0.44	0.66	0.69
$k_{15} = k_{51}$	0.15	0.16	0.22	0.28
k_{22}	0.68	0.70	1.00	0.96
$k_{23} = k_{32}$	0.01	0.02	0.04	0.08
$k_{24} = k_{42}$	0.79	0.81	1.15	1.11
$k_{25} = k_{52}$	0.22	0.21	0.31	0.31
k_{33}	0.42	0.42	0.59	0.63
$k_{34} = k_{43}$	0.32	0.33	0.46	0.49
$k_{35} = k_{53}$	0.30	0.31	0.43	0.45
k_{44}	0.76	0.75	1.08	1.04
$k_{45} = k_{54}$	0.20	0.21	0.31	0.36
k_{55}	0.19	0.20	0.30	0.35

values from the optimization process to the exact values are shown, together with the indication of the standard deviation for each variable. As shown before, the mass and stiffness matrices behave in the same way, and no difference is observed between the two cases. The proposed algorithm is therefore robust with respect to increase of search space.

Lastly, the estimated response computed using the optimized parameters is compared with the target response in Fig. 3. It can be seen that the estimated responses agree very well with the actual ones. Given the similarity between the results of *Case 1* and *Case 2*, only the comparison for *Case 1* is shown.

Overall, very satisfactory results are obtained for the free-noise scenario. It is proven that a big search space does not negatively influence the final result but it is rather a trade-off between the possibility of encountering more local minima and the possibility of exploring more promising paths. Therefore the two cases are comparable. The quality criteria defined in Table 1 in terms of eigenfrequencies deviations are therefore respected.

Table 6. Mean and maximum absolute error on the damping entries of 20 runs for *Case 1* ($\mathbf{x}_{max} = 3\mathbf{x}_*$) and *Case 2* ($\mathbf{x}_{max} = 7\mathbf{x}_*$) in a noise-free scenario

Variable	Mean Value (%)		Max. Value (%)	
	Case 1	*Case 2*	*Case 1*	*Case 2*
c_{11}	0.75063	0.77	1.17	1.30
$c_{12} = c_{21}$	0.91	2.11	2.68	4.60
$c_{13} = c_{31}$	0.76	0.80	1.28	1.24
$c_{14} = c_{41}$	0.62	0.63	0.93	0.96
$c_{15} = c_{51}$	1.44	5.34	5.24	10.30
c_{22}	0.74	1.07	1.35	2.12
$c_{23} = c_{32}$	0.34	0.31	1.25	0.85
$c_{24} = c_{42}$	0.66	0.68	0.98	0.95
$c_{25} = c_{52}$	41.99	84.20	133.48	357.54
c_{33}	0.42	0.43	0.78	0.87
$c_{34} = c_{43}$	0.30	0.23	0.70	0.55
$c_{35} = c_{53}$	0.42	1.06	0.86	2.15
c_{44}	0.74	0.74	1.07	1.02
$c_{45} = c_{54}$	0.20	0.21	0.34	0.37
c_{55}	0.13	0.41	0.48	0.91

Table 7. Damped Problem: Mean and maximum damping and eigenfrequency deviations of 20 runs for *Case 1* ($\mathbf{x}_{max} = 3\mathbf{x}_*$) and *Case 2* ($\mathbf{x}_{max} = 7\mathbf{x}_*$) in a noise-free scenario

Quality Criterion	Mean Value %		Max. Value %	
	Case 1	*Case 2*	*Case 1*	*Case 2*
1st Damp. dev.	0.12	0.12	0.61	0.25
1st Freq. dev.	0.04	0.04	0.07	0.07
2nd Damp. dev.	0.22	0.82	0.84	1.85
2nd Freq. dev.	0.00	0.00	0.00	0.01
3rd Damp. dev.	0.13	0.24	0.27	0.48
3rd Freq. dev.	0.00	0.00	0.00	0.00
4th Damp. dev.	0.06	0.06	0.09	0.14
4th Freq. dev.	0.00	0.00	0.00	0.00
5th Damp. dev.	0.01	0.01	0.02	0.02
5th Freq. dev.	0.00	0.00	0.00	0.00

5.2 Noisy scenario

The hPSO-LS is now tested in a noisy scenario. The input and output (I/O) data are polluted with Gaussian, zero mean, white-noise sequences, whose root mean square (RMS) value is kept to 5%. The noise is added to the absolute accelerations and to the base acceleration. Eq. (11) is used to derive the relative accelerations from the polluted data. The results of the parameters identification are shown in Fig. 4 for *Case 1* and *Case 2*. As expec-

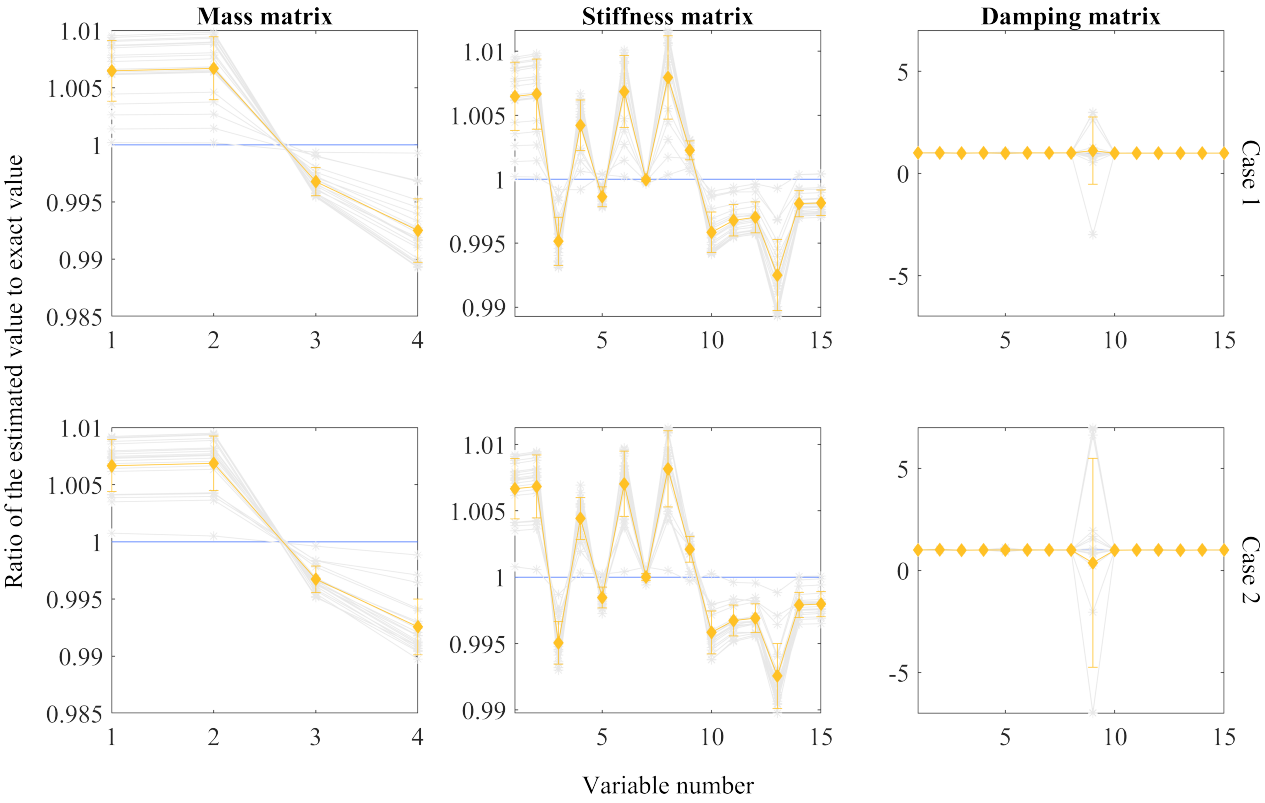

Fig. 2. Results of the identification problem for *Case 1* ($\mathbf{x}_{max} = 3\mathbf{x}_*$) and *Case 2* ($\mathbf{x}_{max} = 7\mathbf{x}_*$) in a noise-free scenario

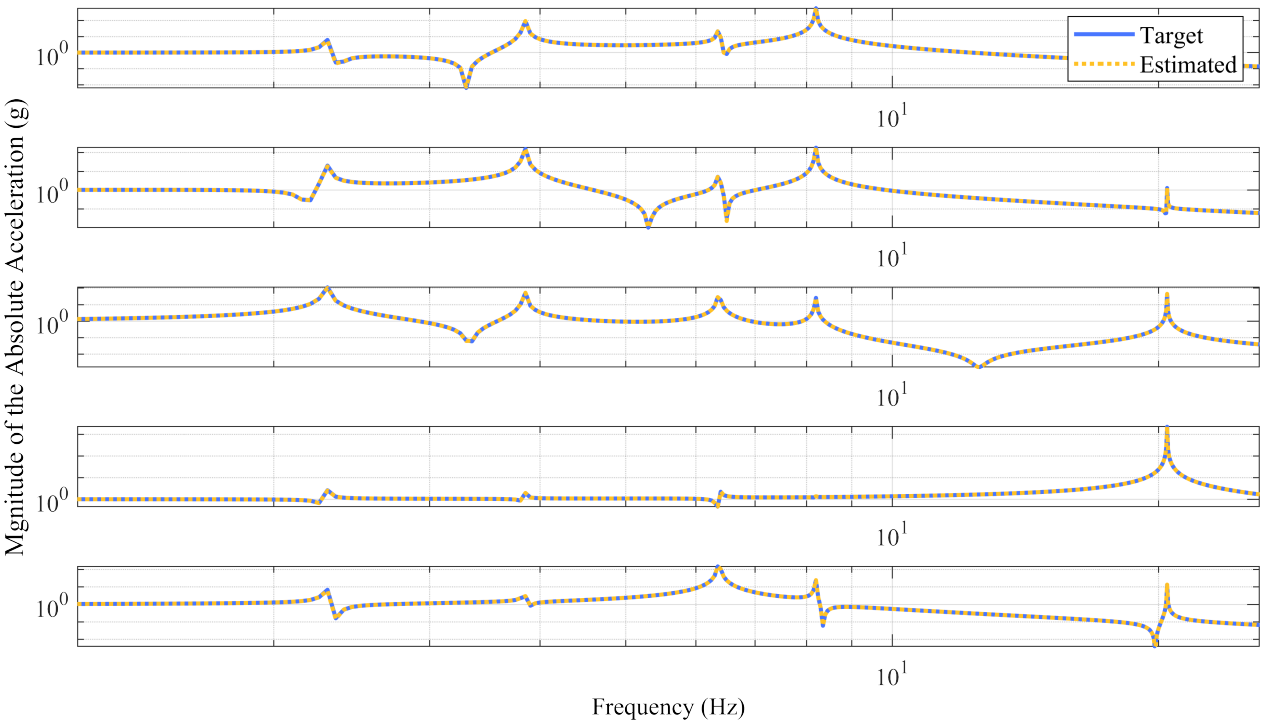

Fig. 3. Comparison of the synthesized absolute acceleration derived from the optimized hPSO-LS solution with the target absolute response for each physical degree of freedom for *Case 1* ($\mathbf{x}_{max} = 3\mathbf{x}_*$) in a noise-free scenario

ted, both the mean and maximum errors of the individual parameters are larger than those in the noise-free scenario. The mean error of the entries varies between 2.59% and 28.53% for the mass matrix, 1.55% and 57.98% for the stiffness matrix and between 0.28% and 212.49% for the damping matrix, for *Case 1*. Similar results increasing the search space, but for the damping entries whose mean errors vary between 5.21% and 497.36%. Although the larger errors on the mass and stiffness matrices compared to the noise-free scenario, the solution of the undamped problem, presented in Table 8, shows a maximum eigenfrequency deviation of 3.38% for *Case 1* and 3.9% for *Case 2*, therefore comparable with the previous results. Different results for the solution of the damped eigenproblem, shown in Table 9. The large error in the damping matrix results in a maximum error on the damping of 21.29% for *Case 1* and 14.78% for *Case 2*. It seems the noisy scenario overestimates the values of the mass matrix, whereas stiffness and damping entries float around the exact values.

In Fig. 5 the comparison between the estimated relative acceleration from the hPSO-LS and the noise-corrupted target response is shown. The noise-free target is also shown to have a full picture of the situation. As it can be seen, a good agreement is achieved in the frequency range of interest. Although the noisy target is given to hPSO-LS, the estimated response seems to follow the noise-free target. It is perfectly possible to match the resonance frequencies in a noisy scenario, as already shown with the solution of the damped and undamped eigenproblem. The larger error compared to the noise-free scenario seems to influence the antiresonance in the low frequency range. Further studies must be conducted to investigate the correlation between this behaviour and matrices' entries.

To conclude with the quality criteria shown in Table 1, the COC and MAC results are shown in Table 10, precisely the worst situation, meaning the biggest off-diagonal terms and the smallest diagonal terms. The solution obtained from the hPSO-LS is in line with the required standard in both a noise-free and noisy scenario. The authors would like to highlight that these comparisons are only possible in this phase, where the capability of hPSO-LS to synthesize a spatial model of a generic structure wants to be investigated.

Given the compliance of the estimated mathematical model with the quality criteria, it is possible to consider its transformation into an CB-equivalent model that includes the modal properties it is intended to keep and the desired physical coordinates. This is intended as the next stage of development of the proposed methodology.

Table 8. Undamped Problem: Mean and maximum eigenfrequency deviations of 20 runs for *Case 1* ($\mathbf{x}_{max} = 3\mathbf{x}_*$) and *Case 2* ($\mathbf{x}_{max} = 7\mathbf{x}_*$) in a noisy scenario

Quality Criterion	Mean Value %		Max. Value %	
	Case 1	*Case 2*	*Case 1*	*Case 2*
1st Freq. dev.	1.16	1.19	3.38	3.90
2nd Freq. dev.	0.74	0.76	0.75	0.95
3rd Freq. dev.	0.01	0.01	0.04	0.04
4th Freq. dev.	0.03	0.02	0.03	0.02
5th Freq. dev.	0.00	0.00	0.00	0.00

Table 9. Damped Problem: Mean and maximum damping and eigenfrequency deviations of 20 runs for *Case 1* ($\mathbf{x}_{max} = 3\mathbf{x}_*$) and *Case 2* ($\mathbf{x}_{max} = 7\mathbf{x}_*$) in a noisy scenario

Quality Criterion	Mean Value %		Max. Value %	
	Case 1	*Case 2*	*Case 1*	*Case 2*
1st Damp. dev.	20.47	14.23	21.29	14.78
1st Freq. dev.	1.16	1.19	3.38	3.90
2nd Damp. dev.	8.94	16.48	9.31	17.81
2nd Freq. dev.	0.74	0.76	0.75	0.95
3rd Damp. dev.	7.59	5.62	7.95	6.46
3rd Freq. dev.	0.01	0.01	0.04	0.04
4th Damp. dev.	1.04	0.97	7.95	7.32
4th Freq. dev.	0.03	0.02	0.03	0.02
5th Damp. dev.	2.96	2.85	3.21	2.95
5th Freq. dev.	0.000	0.00	0.00	0.00

6. Conclusion

A hybrid strategy has been presented for the problem of structural identification of the spatial properties of a 5 DoFs system, knowing the base and the output accelerations. This methodology combines the ability of the APSO to explore possible solutions in the search space, with the final refining of the local search. A healing process has been also introduced to handle physical constraints on the mass and stiffness matrices.

Based on the research work thus far, the following observations and conclusions are drawn:

1. The implementation of the presented algorithm is relatively straightforward. The used cost function does not require the inversion of any matrices, therefore avoiding a possible ill-conditioned situation.

2. The algorithm has been shown to work well in a noise-free scenario, where small errors are observed for the mass, stiffness, and damping variables. Only one entry in the damping matrix shows a large error. The mean maximum errors are 0.87%, 0.62%

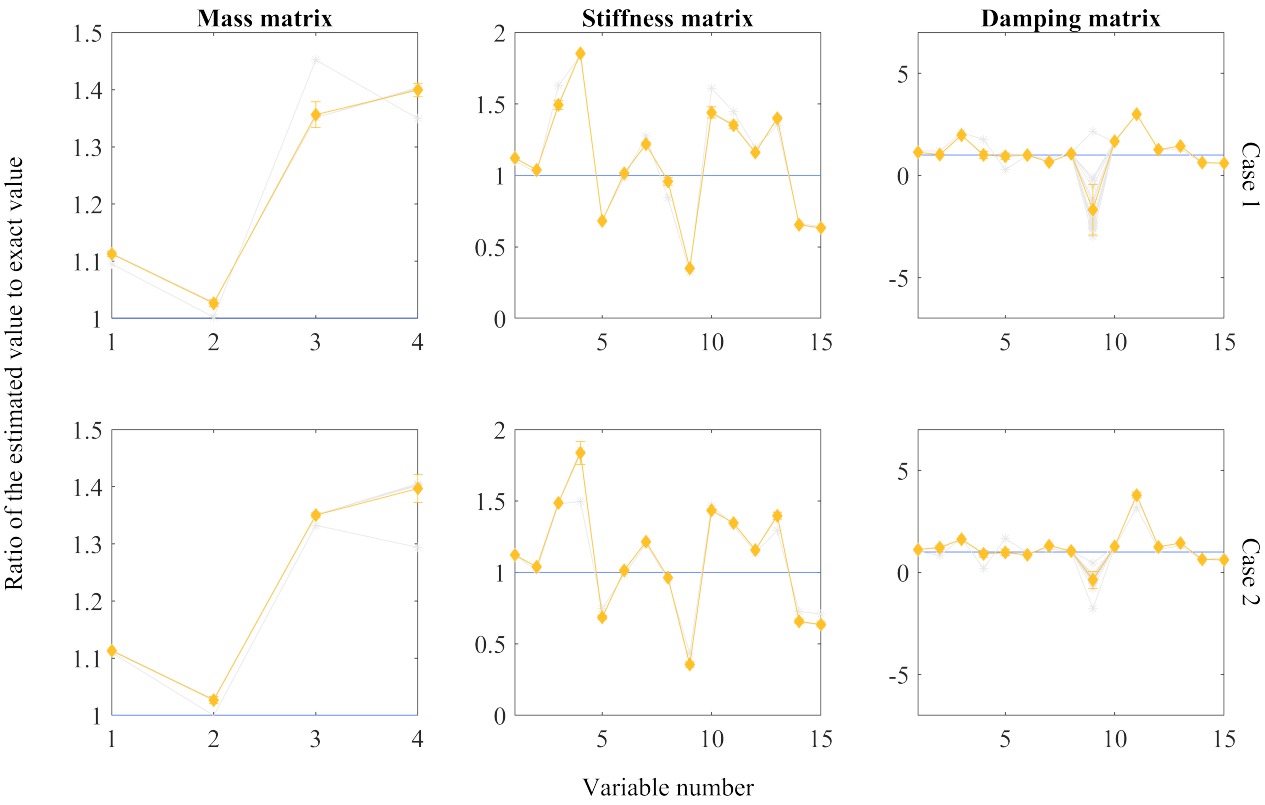

Fig. 4. Results of the identification problem for *Case 1* ($\mathbf{x}_{max} = 3\mathbf{x}_*$) and *Case 2* ($\mathbf{x}_{max} = 7\mathbf{x}_*$) in a noisy scenario

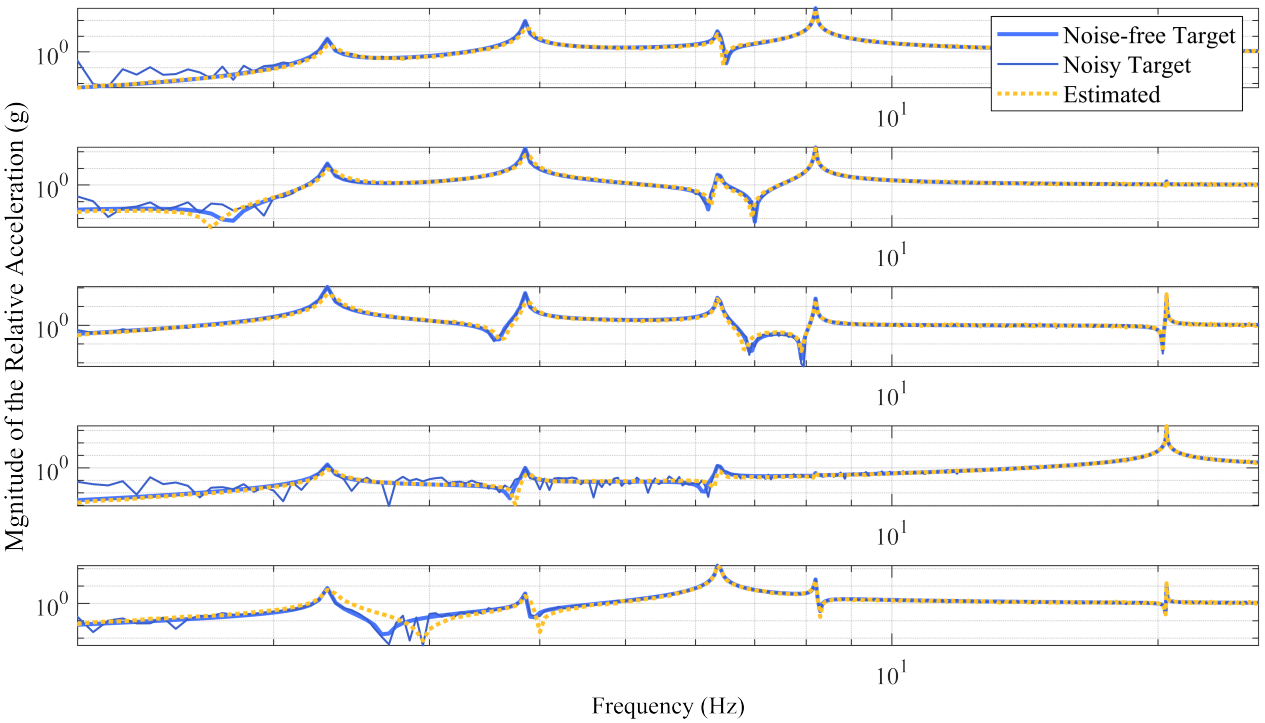

Fig. 5. Comparison of the synthesized relative acceleration derived from the optimized hPSO-LS solution with the noise-free target and noisy target relative response for each physical degree of freedom for *Case 1* ($\mathbf{x}_{max} = 3\mathbf{x}_*$) in a noisy scenario

Table 10. COC and MAC worst result of 20 runs for *Case 1* ($\mathbf{x}_{max} = 3\mathbf{x}_*$) and *Case 2* ($\mathbf{x}_{max} = 7\mathbf{x}_*$) in noise-free and noisy sceneries

	Quality Criterion	*Case 1*		*Case 2*	
		Noise-free	Noisy	Noise-free	Noisy
COC	Smallest diagonal term	1	0.99	1	0.99
	Biggest off-diagonal term	0.00	0.02	0.00	0.01
MAC	Smallest diagonal term	1	0.99	1	0.99
	Biggest off-diagonal term	0.04	0.04	0.04	0.04

and 25.72% for mass, stiffness, and damping. respectively. Both undamped and damped problems present a maximum deviation of the eigenfrequencies of 0.07%. The maximum damping deviation is 1.85%.

3. Although the process is driven by random changes, the results appear robust and converge to the right solution all the times in a noise-free scenario.

4. Adding the noise, the function appears to have more local minima, and therefore the particles might get stuck in those. The check strategy does not always seem to work in this scenario. Further work is underway to improve the numerical efficiency of the method. Although very satisfactory agreements have been achieved regarding modal properties, the spatial properties show large errors. The mean maximum errors are 16.94%, 41.27% and 135%, for mass, stiffness, and damping, respectively. The maximum eigenfrequency and damping deviation is 3.90% and 21.29% respectively.

5. A sensitivity analysis on the search space size has been carried out. As shown, no significant differences in the results have been observed, indicating the potential of getting good results even in a real-case situation, where no prior knowledge of the structure is available, and therefore, large search space must be considered to try to include the global optimum.

References

[1] S. Fransen, "Methodologies for launcher-payload coupled dynamic analysis," *CEAS Space Journal*, vol. 3, no. 1, pp. 13–25, 2012.

[2] J. Young and W. Haile, "Primer on the Craig-Bampton method," *Finite Element Modeling Continuous Improvement, NASA*, 2000.

[3] R. Pintelon and J. Schoukens, *System identification - A Frequency Domain Approach*. John Wiley & Sons, 2010.

[4] G. A. Bekey, "System identification. An introduction and a survey," *Simulation*, vol. 15, no. 4, pp. 151–166, 1970.

[5] R. Isermann, M. Münchhof, R. Isermann, and M. Münchhof, *Identification of Dynamic Systems: An Introduction with Applications*. Springer Science & Business Media, 2010.

[6] R. Eberhart and J. Kennedy, "Particle Swarm Optimization," in *Proceedings of the IEEE international conference on neural networks*, pp. 1942–1948, 1995.

[7] R. Eberhart and J. Kennedy, "New optimizer using particle swarm theory," *Proceedings of the International Symposium on Micro Machine and Human Science*, pp. 39–43, 1995.

[8] C. Elegbede, "Structural reliability assessment based on particles swarm optimization," *Structural Safety*, vol. 27, no. 2, pp. 171–186, 2005.

[9] R. E. Perez and K. Behdinan, "Particle swarm approach for structural design optimization," *Computers and Structures*, vol. 85, no. 19-20, pp. 1579–1588, 2007.

[10] L. J. Li, Z. B. Huang, and F. Liu, "A heuristic particle swarm optimization method for truss structures with discrete variables," *Computers and Structures*, vol. 87, no. 7-8, pp. 435–443, 2009.

[11] A. Kaveh and S. Talatahari, "Particle swarm optimizer, ant colony strategy and harmony search scheme hybridized for optimization of truss structures," *Computers and Structures*, vol. 87, no. 5-6, pp. 267–283, 2009.

[12] S. N. Omkar, D. Mudigere, G. N. Naik, and S. Gopalakrishnan, "Vector evaluated particle swarm optimization (VEPSO) for multi-objective design optimization of composite structures," *Computers and Structures*, vol. 86, no. 1-2, pp. 1–14, 2008.

[13] X. Deng, "System identification based on particle swarm optimization algorithm," *CIS 2009 - International Conference on Computational Intelligence and Security*, vol. 1, pp. 259–263, 2012.

[14] G. Franco, R. Betti, and H. Luş, "Identification of Structural Systems Using an Evolutionary Strategy," *Journal of Engineering Mechanics*, vol. 130, no. 10, pp. 1125–1139, 2004.

[15] C. G. Koh, Y. F. Chen, and C. Y. Liaw, "A hybrid computational strategy for identification of structural parameters," *Computers and Structures*, vol. 81, no. 2, pp. 107–117, 2003.

[16] L. H. Gunderson and L. P. Jr, "Parameter identification of large structural systems in time domain," *Journal of Structural Engineering*, vol. 1, no. 3, pp. 126–145, 2011.

[17] S. Xue, H. Tang, and J. Zhou, "Identification of structural systems using particle swarm optimization," *Journal of Asian Architecture and Building Engineering*, vol. 8, no. 2, pp. 517–524, 2009.

[18] ECSS, *Space Engineering: Modal Survey Assessment*. No. July, ESA Requirements and Standards Division, 2008.

[19] U. Füllekrug, "Utilization of multi-axial shaking tables for the modal identification of structures," *Philosophical Transactions of the Royal Society of London. Series A: Mathematical, Physical and Engineering Sciences*, vol. 359, pp. 1753–1770, 2001.

[20] U. Füllekrug and J. M. Sinapius, "Identification of modal parameters, generalized and effective masses during base-driven tests," *Aerospace Science and Technology*, vol. 2, no. 7, pp. 469–480, 1998.

[21] D. E. Goldberg, *Genetic Algorithms in Search, Optimization and Machine Learning*. Addison-Wesley Longman Publishing Co., Inc., 1st ed., 1989.

[22] G. Yang, "A Modified Particle Swarm Optimizer," in *IEEE international conference on evolutionary computation proceedings. IEEE world congress on computational intelligence (Cat. No. 98TH8360)*, pp. 69–73, 1998.

[23] Y. Shi and R. C. Eberhart, "Empirical study of particle swarm optimization," in *Proceedings of the 1999 Congress on Evolutionary Computation, CEC 1999*, vol. 3, pp. 1945–1950, IEEE, 1999.

[24] R. Poli, J. Kennedy, and T. Blackwell, "Particle swarm optimization - An overview," *Swarm Intelligence*, vol. 1, pp. 33–57, 2007.

[25] J. Kennedy, "The Particle Swarm: Social Adaptation," in *Information Processing Systems*, vol. McGraw-Hil, pp. 303–308, IEEE, 1997.

[26] Z. H. Zhan, J. Zhang, Y. Li, and H. S. Chung, "Adaptive particle swarm optimization," *IEEE Transactions on Systems, Man, and Cybernetics, Part B: Cybernetics*, vol. 39, no. 6, pp. 1362–1381, 2009.

[27] J. Zhang, H. S. H. Chung, and W. L. Lo, "Clustering-based adaptive crossover and mutation probabilities for genetic algorithms," *IEEE Transactions on Evolutionary Computation*, vol. 11, no. 3, pp. 326–335, 2007.

[28] J. Zhan, Zhi-hui and Jing Xiao and Zhang and W. neng Chen, "Adaptive control of acceleration coefficients for particle swarm optimization based on clustering analysis," in *Evolutionary Computation*, pp. 3276–3282, 2007.

[29] J. Byrd, Richard H. and Hribar, Mary E. and Nocedal, "An Interior Point Algorithm for Large-Scale Nonlinear Programming," *SIAM Journal on Optimization*, vol. 9, no. 4, pp. 877–900, 1999.